

Electronic Supplementary Information

Comparing the inherent reactivity of often-overlooked aqueous chlorinating and brominating agents toward salicylic acid

*Matthew A. Broadwater,^{a‡} Tyler L. Swanson,^a John D. Sivey^{*ab}*

^a Department of Chemistry, Towson University, Towson, Maryland, United States

^b Urban Environmental Biogeochemistry Laboratory, Towson University, Towson, Maryland, United States

* E-mail: jsivey@towson.edu; Tel: 1-410-704-6087

‡ Current affiliation: Eshelman School of Pharmacy, University of North Carolina at Chapel Hill, Chapel Hill, North Carolina, United States

Includes 29 pages, 12 tables, and 14 figures

Speciation of Salicylic Acid as a Function of pH

Values corresponding to the first acid dissociation (pK_{a1}) of salicylic acid (SA) in water have been reported in several previous studies and typically fall within the range of 2.9 ± 0.1 (Table S1). Values corresponding to the second acid dissociation (pK_{a2}) of SA have not been reported as extensively in the literature compared to pK_{a1} . Reported values of pK_{a2} range from 12.81 to 13.89 (Table S1). Dudeney and Irving¹ attributed the inconsistencies in measured pK_{a2} values to systematic errors such as the small extent of dissociation to give SA^{2-} in the examined aqueous solutions and the potential for SA^{2-} to undergo chemical decomposition.

Table S1. Literature Reports for Salicylic Acid pK_a Values

Reference	pK_{a1}	pK_{a2}	Comments
2	2.97	13.4	T = 19 °C (pK_{a1}) T = 18 °C (pK_{a2}) <i>Calculations herein are based on these pK_a values.</i>
3	2.93	not reported	T = 25 °C
4	3.0	13.4	not reported
5	2.937	not reported	not reported
6	2.79	not reported	T = 25 °C
7	2.96	not reported	T = 25 °C
8	2.96	not reported	T = 25 °C
9	3.08	not reported	T = 25 °C
1	not reported	13.89 13.74	T = 20 °C T = 25 °C
10	not reported	13.59	T = 25 °C
11	2.81	13.4	T = 25 °C ionic strength = 0.1 M
12	2.827	12.81	T = 25 °C
13	not reported	13.62 ± 0.03	T = 25 °C ionic strength = 0
14	2.97	13.7	T = 25 °C pK_{a2} was described in this reference as "less reliable"

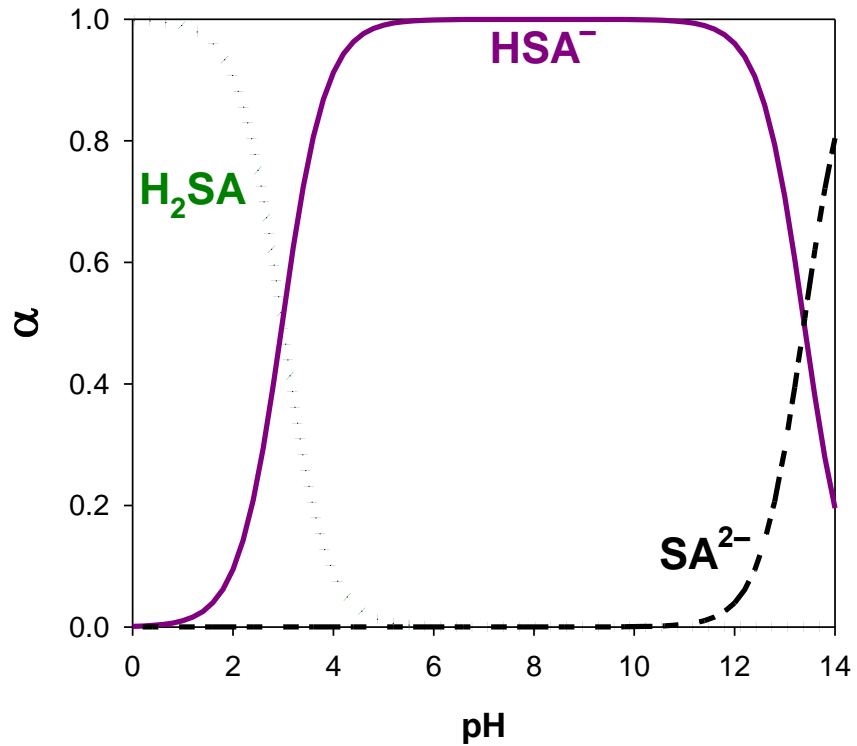


Fig. S1. The fractional composition (α) of salicylic acid as a function of pH. Species shown include the fully protonated acid (H₂SA), hydrogen salicylate (HSA⁻), and salicylate (SA²⁻). The pK_{a1} and pK_{a2} values of 2.97 and 13.4 and ionic strength of 0.1 M were assumed.

Reagents

All reagents were used as received.

Table S2. Reagents, Purity, and Vendor Information

Reagent	Purity or Concentration (wt%)	Vendor
salicylic acid	>99	MP Biomedicals, LLC
3-chlorosalicylic acid	95+	Ark Pharm, Inc
5-chlorosalicylic acid	98	Ark Pharm, Inc
3,5-dichlorosalicylic acid	99	Alfa Aesar
3-bromosalicylic acid	95+	Ark Pharm, Inc
5-bromosalicylic acid	98	Ark Pharm, Inc
3,5-dibromosalicylic acid	97	Acros Organics
methanol	99.9	Fisher Scientific
formic acid	99.5+	Fisher Scientific
acetonitrile	99.9	Fisher Scientific
nitric acid	70	Fisher Scientific
sodium hydroxide (aqueous)	50	Ricca Chemical Company
sodium chloride	99.999	Sigma-Aldrich
sodium bromide	99.5	Acros Organics
sodium nitrate	99	Acros Organics
sodium phosphate dibasic anhydrous	99	Acros Organics
sodium tetraborate decahydrate	99.5	Acros Organics
sodium bicarbonate	99.7+	Acros Organics
sodium hypochlorite (aqueous)	5.65 – 6.00	Fisher Scientific
sodium thiosulfate	≥98	Fisher Scientific

Reactor Compositions and Measured Rate Constants: Chlorination

Solution conditions and pseudo-first-order rate constants for chlorination of SA as a function of pH (Table S3), added sodium chloride (Table S4), and free chlorine (Table S5).

Table S3. Pseudo-First-Order Rate Constants for Formation of 3-CISA ($k_{3\text{-CISA,obs}}$) and 5-CISA ($k_{5\text{-CISA,obs}}$) From Chlorination of SA as a Function of pH at 20 °C^a

pH	$k_{3\text{-CISA,obs}}$ (s ⁻¹)	$k_{5\text{-CISA,obs}}$ (s ⁻¹)
11.14	1.56E-04	1.30E-04
10.87	1.48E-04	1.37E-04
10.66	1.54E-04	1.27E-04
10.50	1.46E-04	1.28E-04
10.41	1.36E-04	1.23E-04
10.17	1.24E-04	1.33E-04
9.86	9.46E-05	1.17E-04
9.53	8.77E-05	1.13E-04
9.23	7.44E-05	1.01E-04
8.93	6.58E-05	8.22E-05
8.60	5.75E-05	7.95E-05
8.26	6.57E-05	9.46E-05
7.92	1.00E-04	1.66E-04
7.59	2.17E-04	4.03E-04
7.37	3.07E-04	5.20E-04
7.06	5.71E-04	1.07E-03
6.78	9.93E-04	1.92E-03
6.51	1.37E-03	2.68E-03
6.22	2.11E-03	4.30E-03

^a All reactors contained: [HOCl]_{tot,o} = 5 mM, borate (19 mM) and carbonate (19 mM) as a mixed pH buffer, [SA]_{tot,o} = 20 μM, [NaCl] = 4.9 mM, [NaNO₃] = 92 mM. All rate constants reported herein of the form 1.14E-04 denote 1.14 × 10⁻⁴.

Table S4. Pseudo-First-Order Rate Constants for Formation of 3-CISA ($k_{3\text{-CISA,obs}}$) and 5-CISA ($k_{5\text{-CISA,obs}}$) From Chlorination of SA as a Function of Chloride Concentration at 20 °C^a

[NaCl] (mM)	$k_{3\text{-CISA,obs}}$ (s ⁻¹)	$k_{5\text{-CISA,obs}}$ (s ⁻¹)
9.87	3.76E-05	4.49E-05
19.8	4.89E-05	6.08E-05
29.6	6.58E-05	7.96E-05
39.5	7.95E-05	9.86E-05

^a All reactors contained: [HOCl]_{tot,o} = 0.46 mM, phosphate (20 mM) as a pH buffer, pH = 6.98, [SA]_{tot,o} = 15 μM, [NaCl] + [NaNO₃] = 100 mM.

Table S5. Pseudo-First-Order Rate Constants for Formation of 3-CISA ($k_{3\text{-CISA,obs}}$) and 5-CISA ($k_{5\text{-CISA,obs}}$) From Chlorination of SA as a Function of Excess Free Chlorine at 20 °C^a

[HOCl] _{tot,o} (μM)	$k_{3\text{-CISA,obs}}$ (s ⁻¹)	$k_{5\text{-CISA,obs}}$ (s ⁻¹)
297	1.02E-05	9.73E-06
397	1.54E-05	1.66E-05
497	1.92E-05	1.76E-05
597	2.42E-05	2.52E-05
697	3.45E-05	3.50E-05
797	4.95E-05	5.55E-05

^a All reactors contained: phosphate (20 mM) as a pH buffer, pH = 7.50, [SA]_{tot,o} = 15 μM, [NaCl] = 9.9 mM, [NaNO₃] = 89 mM.

Example Time Course: Chlorination of SA

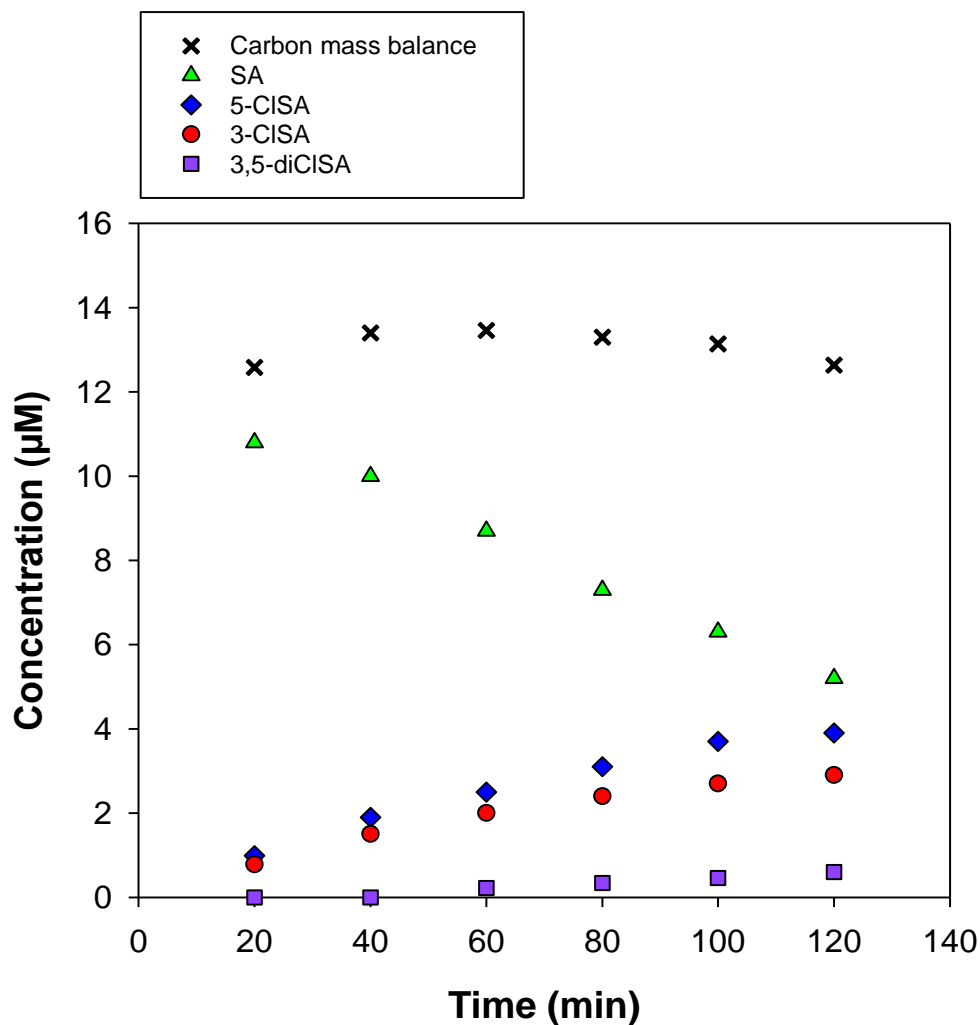


Fig. S2. Example time course of SA reacting with free chlorine to produce 5-CISA and 3-CISA, and 3,5-diCISA. Solution Conditions: $[\text{HOCl}]_{\text{tot},0} = 500 \mu\text{M}$, phosphate (20 mM) as a pH buffer, $\text{pH} = 6.98$, $[\text{SA}]_{\text{tot},0} = 15 \mu\text{M}$, $[\text{NaCl}] = 30 \text{ mM}$, $[\text{NaNO}_3] = 69 \text{ mM}$, $T = 20.0 \text{ }^\circ\text{C}$.

Reactor Compositions and Measured Rate Constants: Bromination

Solution conditions and pseudo-first-order rate constants for bromination of SA as a function of pH (**Table S6**), added sodium chloride (**Table S7**), free chlorine (**Table S8**), added excess bromide (**Table S9**), and added bromide in the presence of excess free chlorine (**Table S10**) are compiled below.

Table S6. Apparent First-Order Rate Constants for Formation 3-BrSA ($k_{3\text{-BrSA,obs}}$) and 5-BrSA ($k_{5\text{-BrSA,obs}}$) From Bromination of SA as a Function of pH at 20 °C^a

pH	$k_{3\text{-BrSA,obs}}$ (s ⁻¹)	$k_{5\text{-BrSA,obs}}$ (s ⁻¹)
9.96	3.67E-05	1.05E-04
9.77	5.19E-05	1.93E-04
9.57	1.00E-04	3.02E-04
9.37	2.18E-04	6.24E-04
9.17	1.80E-04	6.01E-04
9.00	3.25E-04	9.52E-04
8.80	5.46E-04	1.79E-03
8.56	7.97E-04	2.20E-03
8.28	7.46E-04	2.18E-03
8.07	7.91E-04	2.65E-03
7.80	1.03E-03	3.81E-03
7.60	6.43E-04	2.86E-03
7.39	5.89E-04	3.08E-03
7.19	4.41E-04	2.57E-03
6.96	6.64E-04	4.26E-03
6.79	7.58E-04	5.85E-03
6.59	1.03E-03	8.67E-03
6.38	1.39E-03	1.22E-02
6.21	1.87E-03	1.52E-02
6.05	2.59E-03	2.07E-02
5.91	4.03E-03	3.71E-02

^a All reactors contained: [NaBr]_o = 20 μM, [HOCl]_{tot,o} = 27 μM, phosphate (20 mM) or borate (20 mM) or carbonate (20 mM) as a pH buffer, [SA]_{tot,o} = 21 μM, [NaCl] = 4.9 mM, [NaNO₃] = 94 mM.

Table S7. Apparent First-Order Rate Constants for Formation of 3-BrSA ($k_{3\text{-BrSA,obs}}$) and 5-BrSA ($k_{5\text{-BrSA,obs}}$) From Bromination of SA as a Function of Chloride Concentration at 20 °C^a

[NaCl] (mM)	$k_{3\text{-BrSA,obs}}$ (s ⁻¹)	$k_{5\text{-BrSA,obs}}$ (s ⁻¹)
4.93	6.72E-04	3.97E-03
14.8	1.67E-03	1.10E-02
24.6	2.18E-03	1.47E-02
34.4	3.76E-03	2.70E-02

^a All reactors contained: [NaBr]_o = 20 μM, [HOCl]_{tot,o} = 27 μM, phosphate (20 mM) as a pH buffer, pH = 6.96, [SA]_{tot,o} = 20 μM, [NaCl] + [NaNO₃] = 100 mM.

Table S8. Apparent First-Order Rate Constants for Formation of 3-BrSA ($k_{3\text{-BrSA,obs}}$) and 5-BrSA ($k_{5\text{-BrSA,obs}}$) From Bromination of SA as a Function of Excess Free Chlorine at 20 °C^a

[HOCl] _{tot,o} (μM)	$k_{3\text{-BrSA,obs}}$ (s ⁻¹)	$k_{5\text{-BrSA,obs}}$ (s ⁻¹)
91.3	6.94E-04	4.22E-03
183	7.64E-04	4.71E-03
274	8.90E-04	5.48E-03
365	1.05E-03	6.38E-03
457	1.22E-03	7.74E-03

^a All reactors contained: [NaBr]_o = 20 μM, phosphate (20 mM) as a pH buffer, pH = 6.96, [SA]_{tot,o} = 22 μM, [NaCl] = 4.9 mM, [NaNO₃] = 93 mM.

Table S9. Apparent First-Order Rate Constants for Formation of 3-BrSA ($k_{3\text{-BrSA,obs}}$) and 5-BrSA ($k_{5\text{-BrSA,obs}}$) From Bromination of SA as a Function of Bromide Added in Excess of Free Chlorine at 20 °C^a

[NaBr] _o (μM)	$k_{3\text{-BrSA,obs}}$ (s^{-1})	$k_{5\text{-BrSA,obs}}$ (s^{-1})
39.7	6.23E-04	4.72E-03
54.5	9.95E-04	8.03E-03
69.4	1.12E-03	8.78E-03
84.2	1.15E-03	8.43E-03
99.0	1.44E-03	1.18E-02

^a All reactors contained: $[\text{HOCl}]_{\text{tot,o}} = 18 \mu\text{M}$, phosphate (20 mM) as a pH buffer, pH = 7.27, $[\text{SA}]_{\text{tot,o}} = 21 \mu\text{M}$, no added NaCl, $[\text{NaNO}_3] = 94 \text{ mM}$.

Table S10. Apparent First-Order Rate Constants and Calculated Reaction Order in $[\text{HOBr}]_{\text{tot}}$ for Formation of 3-BrSA ($k_{3\text{-BrSA,obs}}$) and 5-BrSA ($k_{5\text{-BrSA,obs}}$) From Bromination of SA as a Function of Added Bromide in the Presence of Excess Free Chlorine at 20 °C^a

$[\text{HOBr}]_{\text{tot,o}}$ (μM)	$k_{3\text{-BrSA,obs}}$ (s^{-1})	$k_{5\text{-BrSA,obs}}$ (s^{-1})	Reaction Order in $[\text{HOBr}]_{\text{tot}}$, n
19.9	7.79E-04	2.17E-03	1.01 ± 0.03
29.7	1.05E-03	3.09E-03	1.02 ± 0.03
39.5	1.89E-03	5.82E-03	1.07 ± 0.04
49.2	2.11E-03	7.78E-03	1.11 ± 0.04
58.8	6.63E-03	1.67E-02	1.22 ± 0.05

^a All reactors contained: $[\text{HOCl}]_{\text{tot,o}} = [\text{NaBr}]_o + 7 \mu\text{M}$, borate (20 mM) as a pH buffer, pH = 8.78, $[\text{SA}]_{\text{tot,o}} = [\text{NaBr}]_o$, $[\text{NaCl}] = 4.9 \text{ mM}$, $[\text{NaNO}_3] = 94 \text{ mM}$.

Example Time Course: Bromination of SA

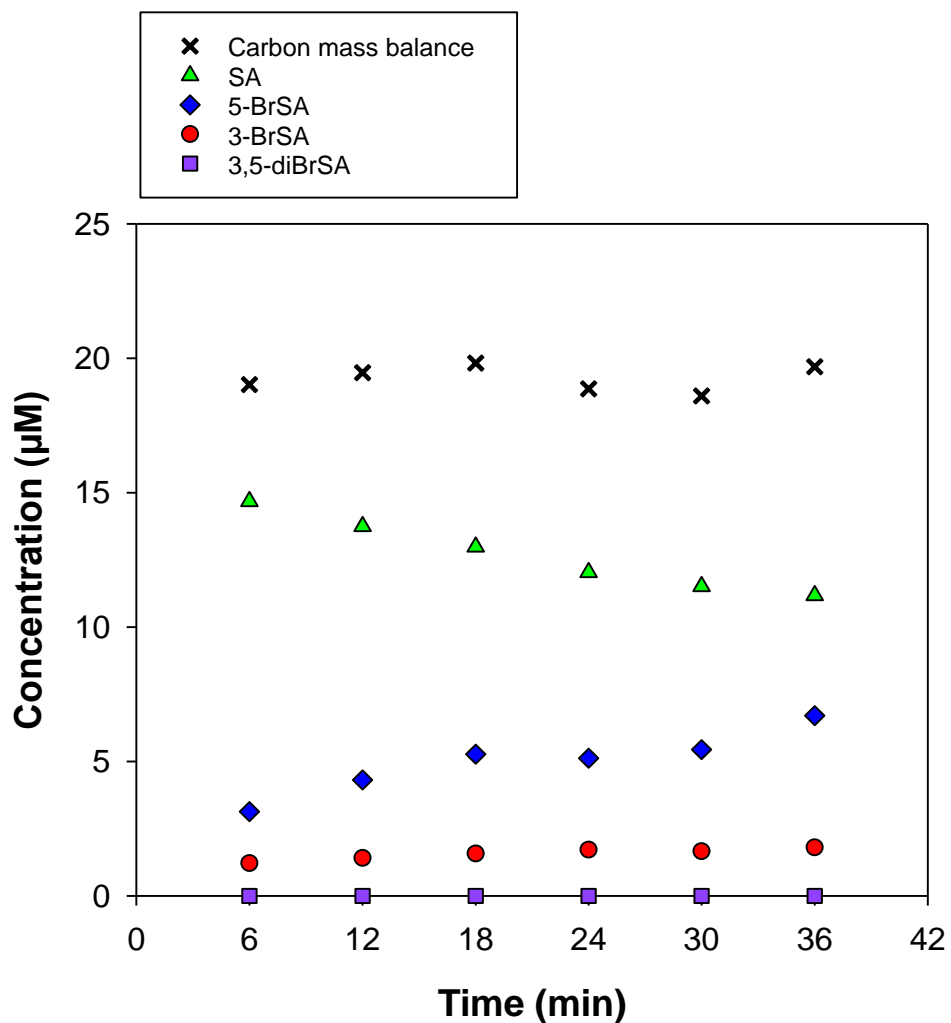


Fig. S3. Example time course of SA reacting with free bromine to produce 5-BrSA, 3-BrSA, and 3,5-diBrSA. Solution Conditions: $[\text{NaBr}]_0 = 20 \mu\text{M}$, $[\text{HOCl}]_{\text{tot},0} = 30 \mu\text{M}$, carbonate (20 mM) as a pH buffer, $\text{pH} = 9.77$, $[\text{SA}]_{\text{tot},0} = 21 \mu\text{M}$, $[\text{NaCl}] = 4.9 \text{ mM}$, $[\text{NaNO}_3] = 94 \text{ mM}$, $T = 20.0 \text{ }^\circ\text{C}$.

Methodological Details: High-Performance Liquid Chromatography

Separations were achieved using an Agilent Poroshell 120 column (50 mm length, 2.1 mm inner diameter, and 2.7 μm particle size) and isocratic elution with a mobile phase consisting of 74 vol% aqueous solution (containing 0.1 vol% formic acid in 18 $\text{M}\Omega\cdot\text{cm}$ water) and 26 vol% acetonitrile. The wavelengths monitored by the diode array detector for signal quantitation were 300 nm (for SA, 3-ClSA, and 3-BrSA) and 313 nm (for 5-ClSA, 5-BrSA, 3,5-diClSA, and 3,5-diBrSA). The elution times of authentic standards of SA, 3-ClSA, 5-ClSA, and 3,5-diClSA were 1.09, 1.57, 2.05, and 2.87 min, respectively. The elution times of authentic standards of 3-BrSA, 5-BrSA, and 3,5-diBrSA were 1.86, 2.41, and 2.86 min, respectively. The total run time was 6.0 min.

Calculation of Rate Constants When [NaBr]₀ Was the Independent Variable

For reactions performed as a function of the initial bromide concentration, bromination rate constants were determined by fitting concentration versus time data for the conversion of SA into 3-bromosalicylate (3-BrSA) and 5-bromosalicylate (5-BrSA) according to eqn (12) – (15) in the main text and repeated here:

$$\frac{d[\text{SA}]_{\text{tot}}}{dt} = -(k_{3\text{-BrSA,app}} + k_{5\text{-BrSA,app}})[\text{SA}]_{\text{tot}}[\text{HOBr}]_{\text{tot}}^n \quad (12)$$

$$\begin{aligned} \frac{d[3\text{-BrSA}]_{\text{tot}}}{dt} = & k_{3\text{-BrSA,app}}[\text{SA}]_{\text{tot}}[\text{HOBr}]_{\text{tot}}^n \\ & - k'_{3\text{-BrSA,app}}[3\text{-BrSA}]_{\text{tot}}[\text{HOBr}]_{\text{tot}}^n \end{aligned} \quad (13)$$

$$\begin{aligned} \frac{d[5\text{-BrSA}]_{\text{tot}}}{dt} = & k_{5\text{-BrSA,app}}[\text{SA}]_{\text{tot}}[\text{HOBr}]_{\text{tot}}^n \\ & - k'_{5\text{-BrSA,app}}[5\text{-BrSA}]_{\text{tot}}[\text{HOBr}]_{\text{tot}}^n \end{aligned} \quad (14)$$

$$\begin{aligned} \frac{d[\text{HOBr}]_{\text{tot}}}{dt} = & -(k_{3\text{-BrSA,app}} + k_{5\text{-BrSA,app}})[\text{SA}]_{\text{tot}}[\text{HOBr}]_{\text{tot}}^n \\ & - k'_{3\text{-BrSA,app}}[3\text{-BrSA}]_{\text{tot}}[\text{HOBr}]_{\text{tot}}^n \\ & - k'_{5\text{-BrSA,app}}[5\text{-BrSA}]_{\text{tot}}[\text{HOBr}]_{\text{tot}}^n \end{aligned} \quad (15)$$

Scientist 3.0 (MicroMath Scientific Software) was used to simultaneously solve the system of differential equations represented by eqn (12) – (15). Time, [SA], [3-BrSA], and [5-BrSA] were treated as model input. Apparent rate constants corresponding to formation ($k_{3\text{-BrSA,app}}$, $k_{5\text{-BrSA,app}}$) and loss ($k'_{3\text{-BrSA,app}}$, $k'_{5\text{-BrSA,app}}$) of 3-BrSA and 5-BrSA, as well as the reaction order in [HOBr]_{tot} (i.e., n) were treated as fitting parameters. Initial ($t = 0$) conditions were specified based on calculated, initial concentrations of the respective reagents. To improve the precision of the calculated fitting parameters, the following iterative modeling approach was employed:

- 1) Rate constants corresponding to loss of 3-BrSA and 5-BrSA were fixed at 0, n was fixed at 1, and best-fit values of $k_{3\text{-BrSA,app}}$ and $k_{5\text{-BrSA,app}}$ were calculated.
- 2) Previously determined values of $k_{3\text{-BrSA,app}}$ and $k_{5\text{-BrSA,app}}$ were fixed, and best-fit values of $k'_{3\text{-BrSA,app}}$ and $k'_{5\text{-BrSA,app}}$ were calculated.

- 3) Previously determined values of $k_{3-\text{BrSA,app}}$, $k_{5-\text{BrSA,app}}$, $k'_{3-\text{BrSA,app}}$, and $k'_{5-\text{BrSA,app}}$ were fixed, and a best-fit value of n was calculated.
- 4) Previously determined values of $k'_{3-\text{BrSA,app}}$, $k'_{5-\text{BrSA,app}}$, and n were fixed, and best-fit values of $k_{3-\text{BrSA,app}}$ and $k_{5-\text{BrSA,app}}$ were calculated.
- 5) Steps 2 – 4 were repeated until all fitting parameters were optimized (indicated by $< 5\%$ relative change in values from one iteration to the next).

Effects of Buffer Concentration on Chlorination of SA

The influence of the formal concentrations of pH buffers on pseudo-first-order rate constants of SA chlorination are shown below for phosphate (Fig. S4), borate (Fig. S5), and carbonate (Fig. S6).

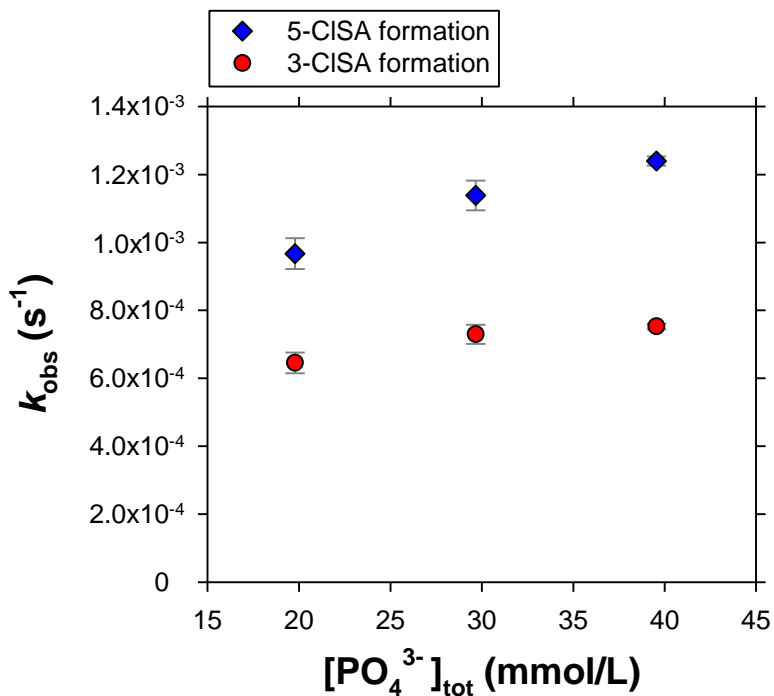


Fig. S4. Pseudo-first-order rate constants (k_{obs}) for chlorination of salicylic acid yielding 5-chlorosalicylic acid (5-CISA) and 3-chlorosalicylic acid (3-CISA) as a function of the total phosphate concentration. Error bars denote 95% confidence intervals (smaller than symbols where not shown). Conditions: $[\text{HOCl}]_{\text{tot},0} = 4.57$ mM, $\text{pH} = 7.4$, $[\text{NaCl}] = 5.0$ mM, $[\text{NaNO}_3] = 94$ mM, $[\text{SA}]_{\text{tot},0} = 21$ μM , $T = 20.0$ $^{\circ}\text{C}$.

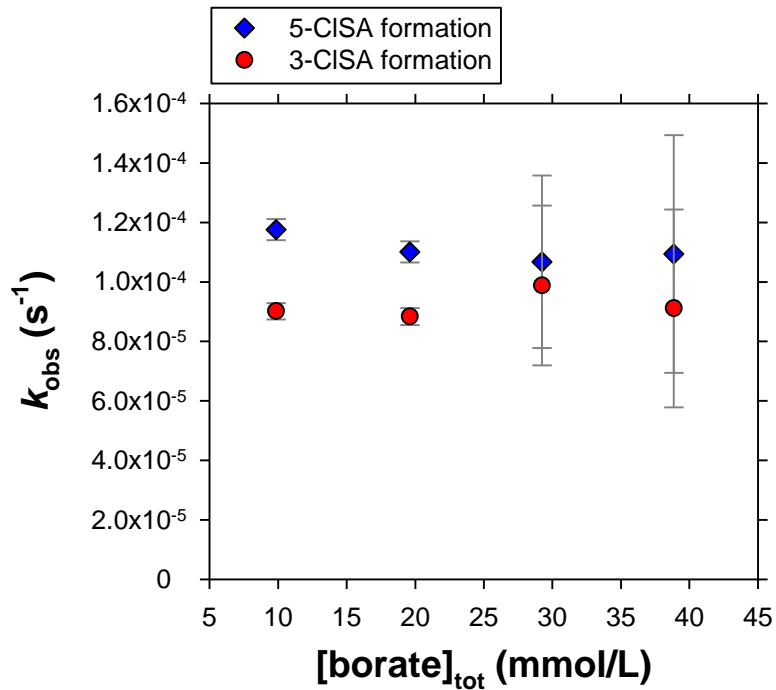


Fig. S5. Pseudo-first-order rate constants (k_{obs}) for chlorination of salicylic acid yielding 5-chlorosalicylic acid (5-CISA) and 3-chlorosalicylic acid (3-CISA) as a function of the total borate concentration. Error bars denote 95% confidence intervals. Conditions: $[HOCl]_{tot,0} = 5.0$ mM, pH = 9.6, $[NaCl] = 4.9$ mM, $[NaNO_3] = 93$ mM, $[SA]_{tot,0} = 21$ μ M, $T = 20.0$ $^{\circ}$ C.

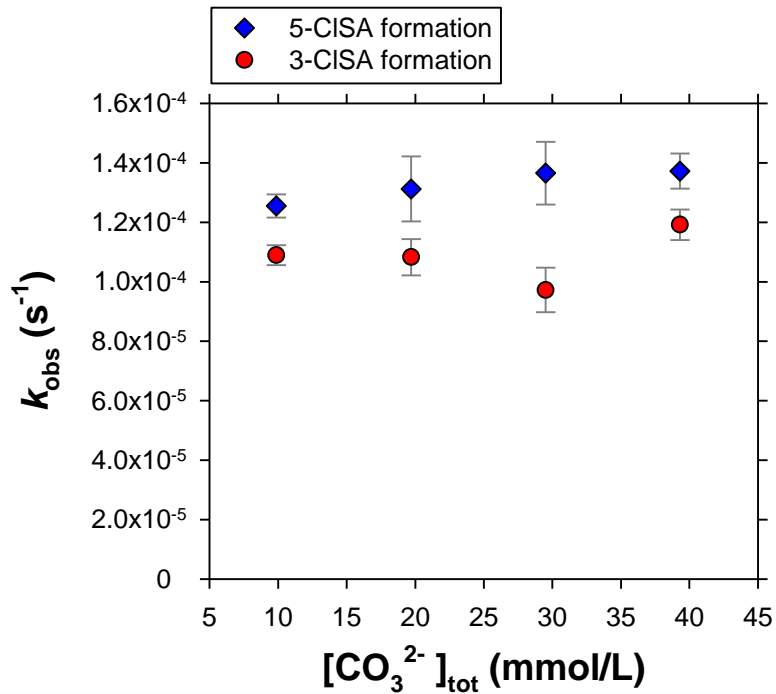


Fig. S6. Pseudo-first-order rate constants (k_{obs}) for chlorination of salicylic acid yielding 5-chlorosalicylic acid (5-CISA) and 3-chlorosalicylic acid (3-CISA) as a function of the total carbonate concentration. Error bars denote 95% confidence intervals. Conditions: $[\text{HOCl}]_{\text{tot},0} = 5.0$ mM, $\text{pH} = 9.6$, $[\text{NaCl}] = 4.9$ mM, $[\text{NaNO}_3] = 94$ mM, $[\text{SA}]_{\text{tot},0} = 21$ μM , $T = 20.0$ $^{\circ}\text{C}$.

Effects of Buffer Identity on Chlorination of SA

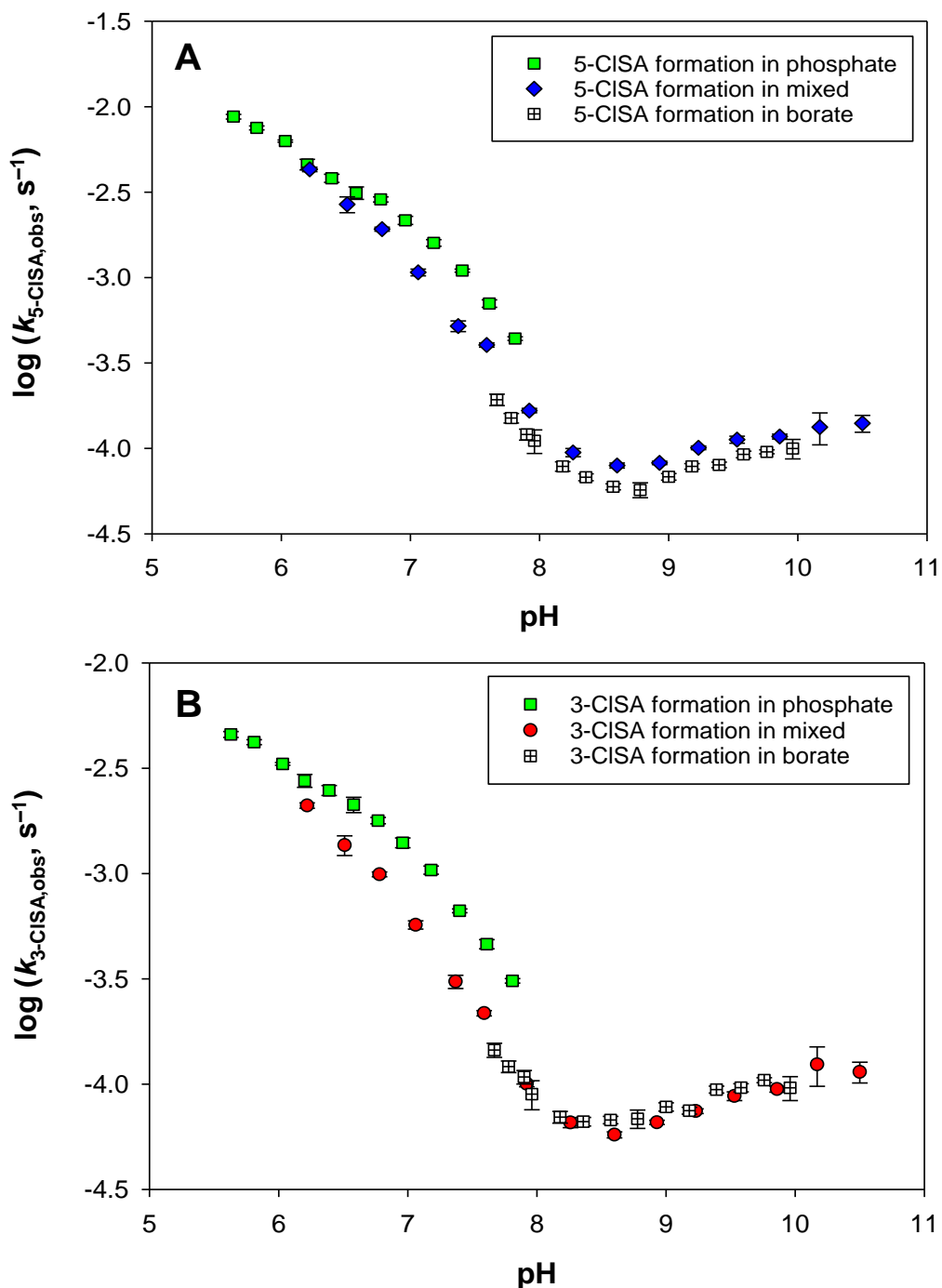


Fig. S7. Formation of (A) 5-chlorosalicylic acid (5-CISA), and (B) 3-chlorosalicylic acid (3-CISA), in a phosphate only, borate only, and mixed (borate + carbonate) buffer system. Error bars denote 95% confidence intervals (smaller than symbols if not shown). Conditions for both frames: $[\text{HOCl}]_{\text{tot},0} = 5.0 \text{ mM}$, formal concentration of each buffer component = 20 mM, $[\text{SA}]_{\text{tot},0} = 20 \text{ }\mu\text{M}$, $[\text{NaCl}] = 4.9 \text{ mM}$, $[\text{NaNO}_3] = 92 \text{ mM}$, $T = 20.0 \text{ }^\circ\text{C}$. Data from the mixed buffer system are identical to those shown in Fig. 1 (main text).

Effects of Total Phosphate Concentration on Bromination of SA

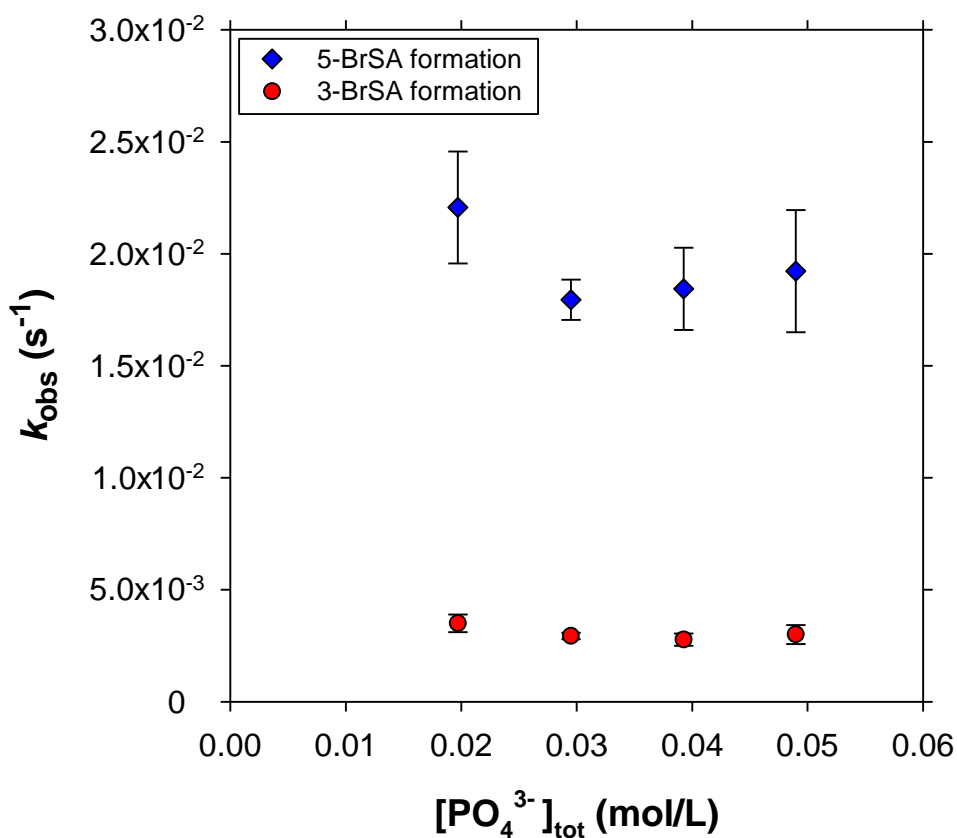


Fig. S8. Pseudo-first-order rate constants for bromination of salicylic acid as a function of the total phosphate concentration. Error estimates denote 95% confidence intervals (smaller than symbols if not shown). Conditions: $[\text{HOCl}]_{\text{tot},0} = 27 \mu\text{M}$, $\text{pH} = 7.01$, $[\text{NaBr}] = 20 \mu\text{M}$, $[\text{NaCl}] = 4.9 \text{ mM}$, $[\text{NaNO}_3] = 94 \text{ mM}$, $[\text{SA}]_{\text{tot},0} = 21 \mu\text{M}$, $T = 20.0 \text{ }^\circ\text{C}$.

Effects of Excess Bromide Concentration on Bromination of SA

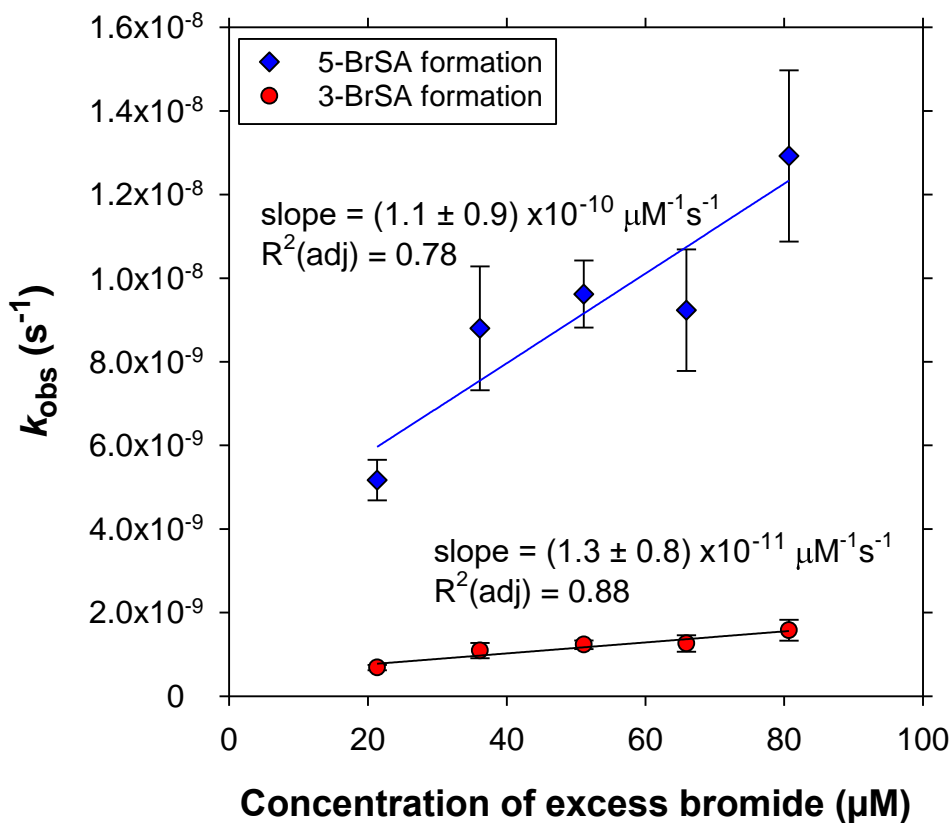


Fig. S9. Pseudo-first-order bromination rate constants as a function of excess bromide, calculated as $[NaBr] - [HOCl]_{tot,o}$. Uncertainties denote 95% confidence intervals (smaller than symbols if not shown). Conditions: $[HOCl]_{tot,o} = 18 \mu M$, phosphate (20 mM) as a pH buffer, pH = 7.3, $[SA]_{tot,o} = 20 \mu M$, no added NaCl, $[NaNO_3] = 94 \text{ mM}$, $T = 20.0 \text{ }^\circ C$.

Effects of the Initial Concentration of SA on Bromination Rates

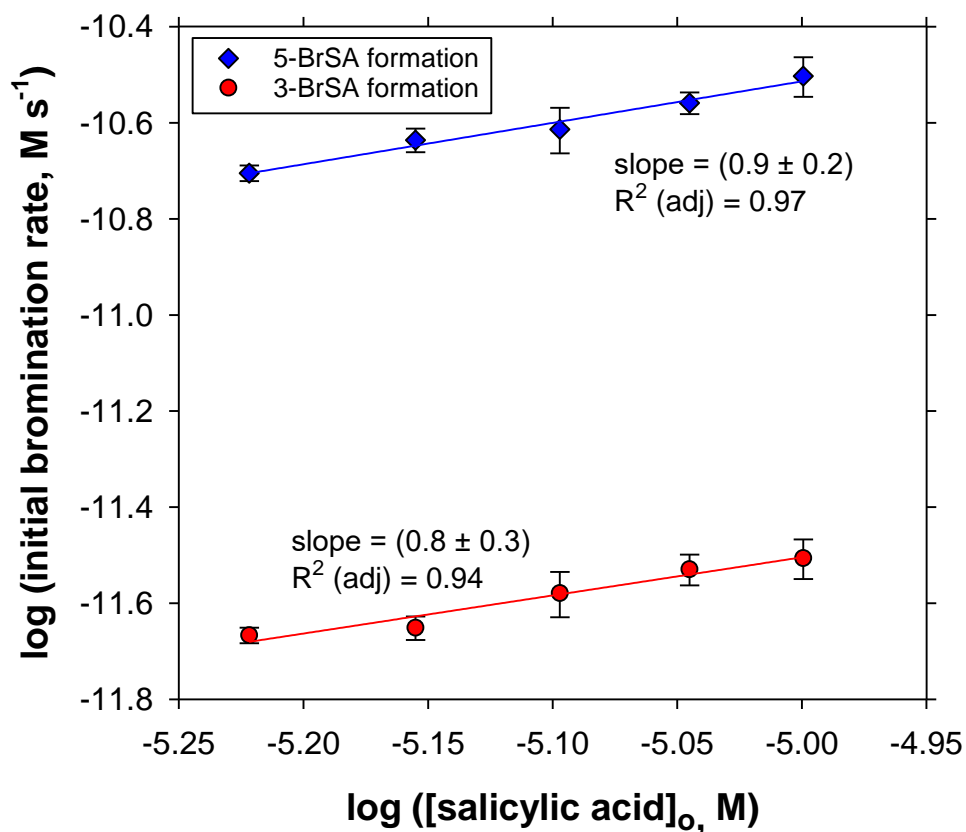


Fig. S10. Initial rates of formation of 5-bromosalicylate (5-BrSA) and 3-bromosalicylate (3-BrSA) as a function of the total initial concentration of SA; note log scale on both axes. Uncertainties denote 95% confidence intervals. Conditions: [HOCl]_{tot,0} = 100 μM, phosphate (20 mM) as a pH buffer, pH = 7.2, [NaBr] = 100 μM, [NaCl] = 5 mM, [NaNO₃] = 95 mM, *T* = 20.0 °C.

Alternative Chlorination Models

Model fits to experimental data assuming various combinations of possible chlorinating agents reacting with hydrogen salicylate are depicted in Figure S11. Model fits assuming two possible nucleophiles (hydrogen salicylate and salicylate) are shown in Figure S12.

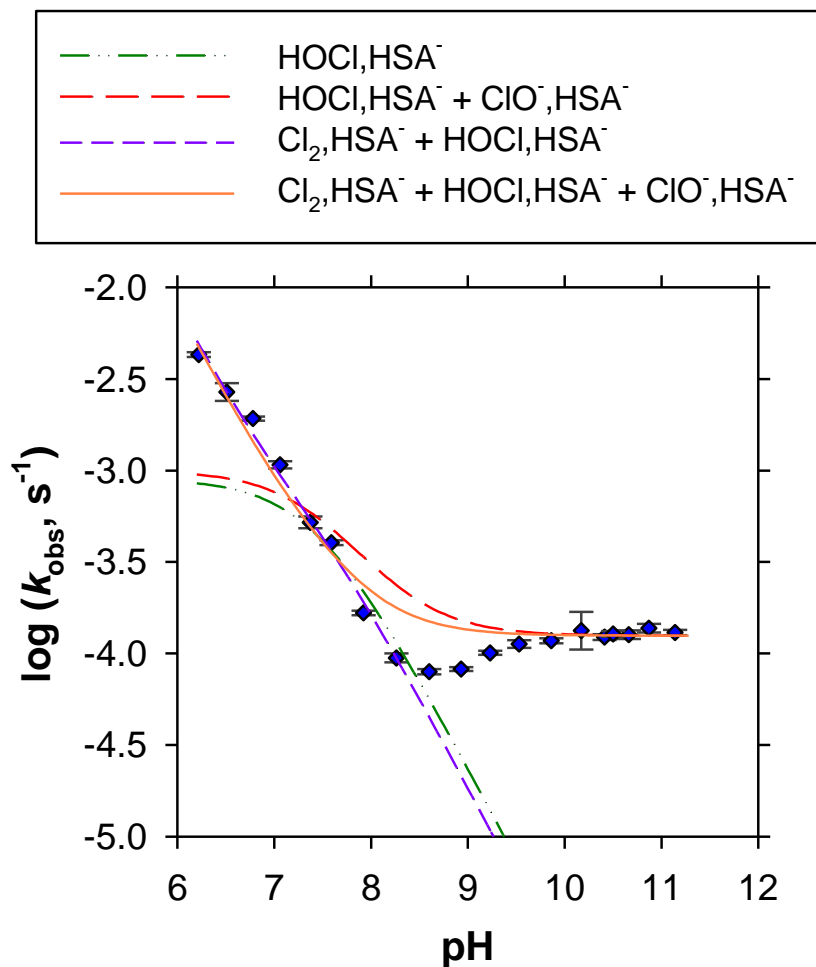


Fig. S11. Alternative model fits (lines) for chlorination of SA compared to experimentally measured k_{obs} values (blue diamonds); for clarity, only data corresponding to the formation of 5-chlorosalicylate are shown. Each of the models assumes hydrogen salicylate (HSA⁻) is the sole nucleophile. Error bars denote 95% confidence intervals (smaller than symbols if not shown). A model considering HOCl, ClO⁻, Cl₂, and Cl₂O (not shown) provides a similar fit as the Cl₂ + HOCl + ClO⁻ model (orange line). Conditions: [HOCl]_{tot,o} = 5 mM, borate (19 mM) and carbonate (19 mM) as a mixed pH buffer, [SA]_{tot,o} = 20 μM, [NaCl] = 4.9 mM, [NaNO₃] = 92 mM, $T = 20.0$ °C.

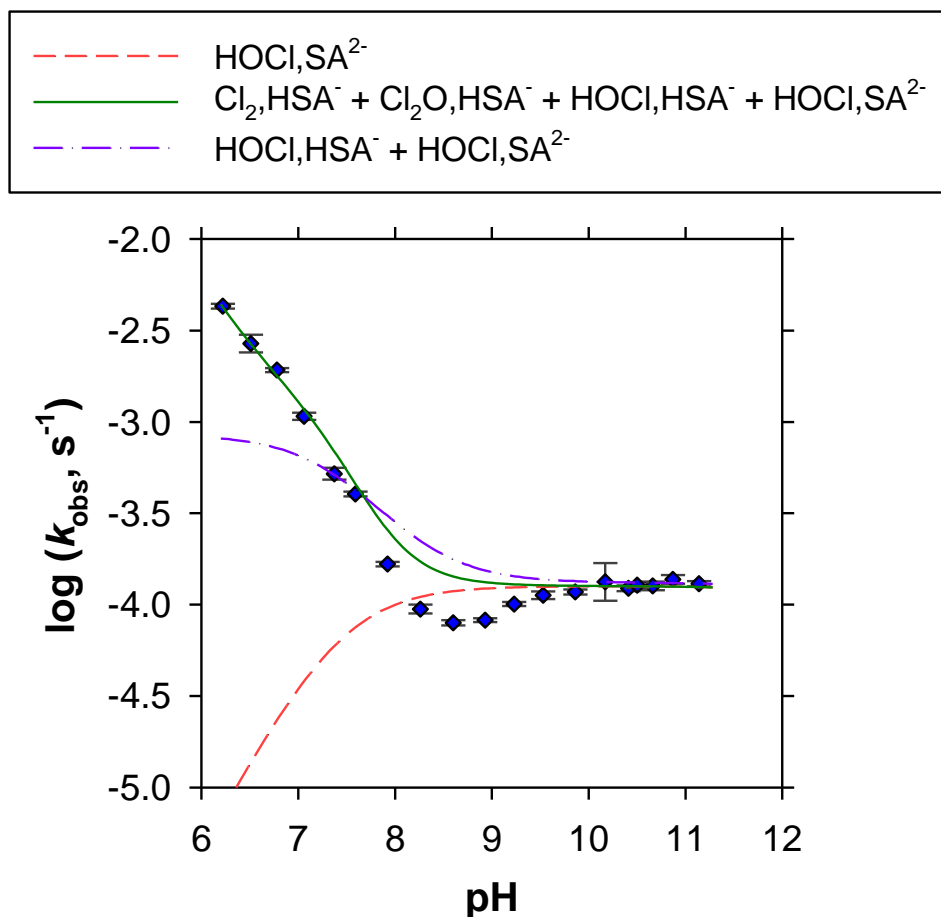


Fig. S12. Alternative model fits (lines) for chlorination of SA compared to experimentally measured k_{obs} values (blue diamonds); for clarity, only data corresponding to the formation of 5-chlorosalicylate are shown. Nucleophiles include hydrogen salicylate (HSA⁻) and salicylate (SA²⁻). Error bars denote 95% confidence intervals (smaller than symbols if not shown). Conditions: [HOCl]_{tot,0} = 5 mM, borate (19 mM) and carbonate (19 mM) as a mixed pH buffer, [SA]_{tot,0} = 20 μM, [NaCl] = 4.9 mM, [NaNO₃] = 92 mM, $T = 20.0$ °C.

Alternative Bromination Models

Model fits to experimental data assuming BrCl only or HOBr only reacting with hydrogen salicylate are depicted in Figure S13.

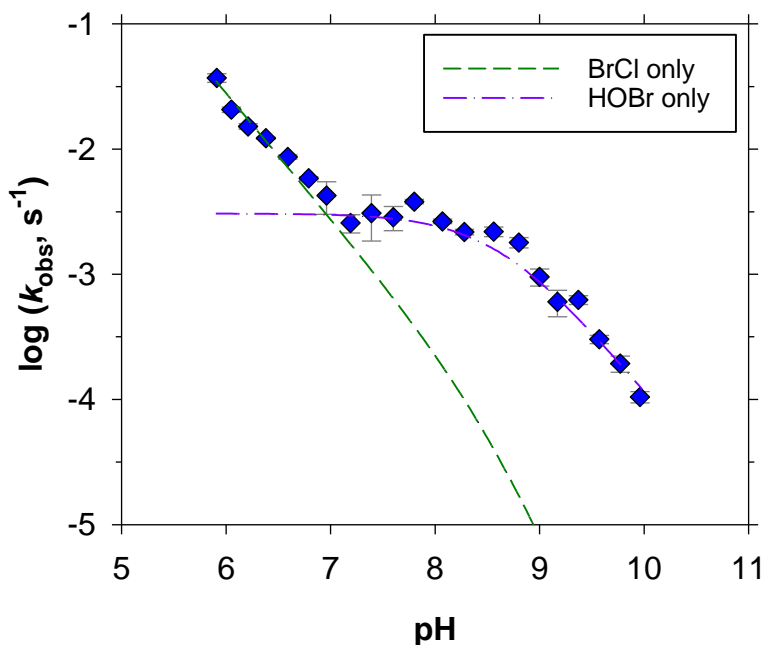


Fig. S13. Alternative model fits (lines) for bromination of SA compared to experimentally measured k_{obs} values (blue diamonds); for clarity, only data corresponding to the formation of 5-bromosalicylate are shown. Each of the models assumes hydrogen salicylate (HSA^-) is the sole nucleophile. Error bars denote 95% confidence intervals (smaller than symbols if not shown). Conditions: $[\text{NaBr}]_0 = 20 \mu\text{M}$, $[\text{HOCl}]_{\text{tot},0} = 27 \mu\text{M}$, a pH buffer (20 mM formal concentration of phosphate, borate, or carbonate), $[\text{SA}]_{\text{tot},0} = 21 \mu\text{M}$, $[\text{NaCl}] = 4.9 \text{ mM}$, $[\text{NaNO}_3] = 94 \text{ mM}$, $T = 20.0 \text{ }^\circ\text{C}$.

Determination of Rate Constants Specific to Individual Halogenating Agents

Halogenating agent-specific second-order rate constants were obtained via iterative least-squares regression analyses of eqn (24) and (25) (main text) for chlorination and bromination, respectively. This approach is based on the method reported in several previous kinetic studies involving chlorination and bromination.¹⁵⁻¹⁹ The bins used to increase the precision of the fitting procedure are shown in Tables S11 (for chlorination) and S12 (for bromination). These bins are used to isolate the data that are most likely to be influenced by the specific halogenating agent under consideration.

Table S11. Bins Used While Performing Nonlinear Regression Analysis to Determine Rate Constants Specific to Individual Chlorinating Agents

Optimization Order ^a	Fitting Parameters ^b	Nucleophile	Input Data ^c
1	$K_{a,SAOCl}$ and J	salicyloyl hypochlorite (phenolate form)	Table S3 (pH > 8.8 only)
2	k_{HOCl}	hydrogen salicylate	Table S3 (7.7 < pH < 9.5 only)
3	k_{Cl_2} and k_{Cl_2O}	hydrogen salicylate	Table S3 (pH < 8.0 only)

^a Iterations were performed following the order of optimization until values of fitting parameters varied by < 5% in subsequent iterations. The same order of optimization was followed when determining values of fitting parameter associated with formation of 3-CISA and 5-CISA.

^b $K_{a,SAOCl}$ denotes the acid-dissociation constant of salicyloyl hypochlorite (phenolic form). J is a composite coefficient which accounts for (1) the equilibrium constant corresponding to the formation of salicyloyl hypochlorite from the reaction of hydrogen salicylate with free chlorine, and (2) the reactivity of salicyloyl hypochlorite toward chlorination by free chlorine. The value of the equilibrium constant corresponding to formation of salicyloyl hypochlorite is unknown, which precludes the calculation of a second-order rate constant corresponding to formation of 3-CISA and 5-CISA from the putative intermediate salicyloyl hypochlorite. Determination of J does permit, however, estimates of the relative contribution of the salicyloyl hypochlorite pathway to overall chlorination rates of SA.

^c The data in Table S4 (with $[Cl^-]$ as the independent variable) can conceivably be used as input when determining k_{Cl_2} . For experiments performed as a function of $[Cl^-]$, plots of k_{obs} versus $[Cl^-]$ are generally linear (Fig. 2). For these plots, the contribution of Cl_2 is associated with the slope, and the contributions of all other active halogenating agents are associated in aggregate with the y-intercept (for a mathematical treatment of these relationships, see ref 17). Relying on these data sets can, however, hamper modeling efforts due to the need to group the reactivity of multiple species (e.g., HOCl and Cl_2O) into a single (extrapolated) term (the y-intercept). Similar issues can arise if data obtained as a function of $[HOCl]_{tot,o}$ are used as input when determining values of k_{HOCl} and k_{Cl_2O} , depending on the linearity of such plots and the uncertainty inherent in the y-intercepts.

Table S12. Bins Used While Performing Nonlinear Regression Analysis to Determine Rate Constants Specific to Individual Brominating Agents ^a

Fitting Parameter	3-BrSA ^b	5-BrSA ^c
k_{BrCl}	Table S6 (pH < 7.0 only)	Table S6 (pH < 7.0 only)
k_{BrOCl}	Table S8	Table S8
$k_{\text{Br}_2\text{O}}$		Table S6 (pH > 7.8 only)
k_{HOBr}	Table S6 (pH > 9.0 only)	Table S6 (pH > 9.0 only)
k_{Br_2}	Table S9	Table S9

^a All bromination rate constants herein assume hydrogen salicylate as the reactive nucleophile. Inclusion of terms for alternative nucleophiles (e.g., dibasic salicylate, salicyloyl hypohalites) did not improve model fits. The data shown in Table S7 (with [Cl⁻] as the independent variable) can conceivably be used as input data when determining k_{BrCl} . For experiments performed as a function of [Cl⁻], plots of k_{obs} versus [Cl⁻] are generally linear (Fig. 6). For these plots, the contribution of BrCl is associated with the slope, and the contributions of all other active halogenating agents are associated in aggregate with the y-intercept (for a mathematical treatment of these relationships, see ref 15). Relying on these data sets can hamper efforts to quantify second-order rate constants due to the need to group the reactivity of multiple species (e.g., HOBr, Br₂O, BrOCl) into a single (extrapolated) term (the y-intercept).

^b Order of optimization: BrCl, BrOCl concurrent with Br₂O, followed by iterations in this order until best-fit second-order rate constants converged, and then best-fit values were obtained for HOBr and Br₂.

^c Order of optimization: HOBr, Br₂O, BrOCl, followed by iterations in this order until best-fit second-order rate constants converged, and then best-fit values were obtained for BrCl and Br₂.

Fractional Contributions of Individual Halogenating Agents

The fractional contribution (f_X) of an individual halogenating agent (X) can be calculated as:

$$f_X = \frac{k_X[X]}{k_{Cl,obs} + k_{Br,obs}} \quad (S1)$$

where k_X and $[X]$ denote the second-order rate constant and molar concentration of halogenating agent X; $k_{Cl,obs}$ and $k_{Br,obs}$ correspond to pseudo-first-order rate constants for chlorination and bromination, which can be determined via eqn (24) and eqn (25) in the main text, respectively. To determine the fractional contribution of salicyloyl hypochlorite to net halogenation rates, the numerator in eqn (S1) would be replaced with $J \frac{K_{a,SAOCl}}{K_{a,SAOCl} + 10^{-pH}} [HOCl]_{tot}^2$. Predicted values of f_X for halogenation of SA in bromide-containing waters treated with free chlorine are shown in Figure S14.

Eqn (S1) is best viewed as the fractional contribution of a halogenating agent to the *initial* rate of halogenation (chlorination + bromination), noting that f_X can change over the course of a reaction as reactants are consumed. Eqn (S1) assumes that the hypothetical solution has a temperature of 20 °C and that the speciation of free chlorine and free bromine is thermodynamically-controlled (i.e., formation of active halogenating agents is assumed not to limit rates of halogenation).

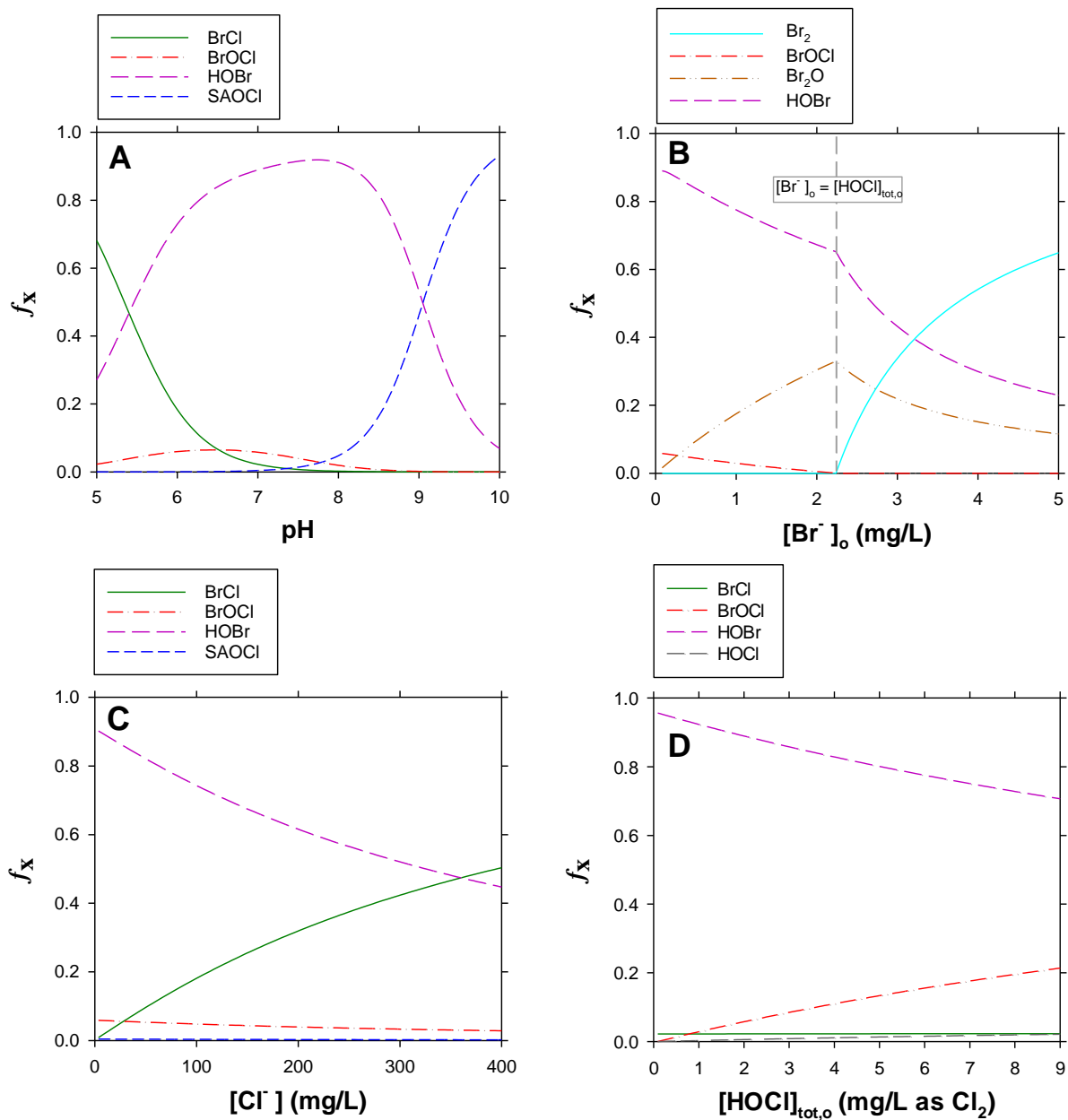


Fig. S14. Fractional contributions (f_x) of individual halogenating agents toward net halogenation (chlorination + bromination) rates of SA as a function of (A) pH, (B) $[\text{Br}^-]_o$, (C) $[\text{Cl}^-]$, and (D) $[\text{HOCl}]_{\text{tot},o}$. For clarity, only the four halogenating agents that contribute most to overall halogenation rates are shown in each frame. Unless otherwise indicated on the x-axes, the conditions are typical of chlorinated drinking water: pH = 7.0, $[\text{Br}^-] = 0.10$ mg/L (1.25 μM), $[\text{Cl}^-] = 11$ mg/L (0.30 mM), $[\text{HOCl}]_{\text{tot},o} = 2.0$ mg/L as Cl_2 (28 μM), and $T = 20$ °C.

References

1. A. W. L. Dudeney and R. J. Irving, *J. Chem. Soc. Farad. Trans. 1*, 1975, **71**, 1215-1220.
2. D. Lide, ed., *Handbook of Chemistry and Physics*, CRC Press, Boca Raton, 1996.
3. L. Geiser, Y. Henchoz, A. Galland, P.-A. Carrupt and J.-L. Veuthey, *J. Sep. Sci.*, 2005, **28**, 2374-2380.
4. A. C. Moffat, J. V. Jackson, M. S. Moss, B. Widdop and E. S. Greenfield, *Clarke's Isolation and Identification of Drugs*, The Pharmaceutical Press, London, 2nd edn., 1986.
5. T. Hirokawa, M. Nishino and Y. Kiso, *J. Chrom. A*, 1982, **252**, 49-65.
6. G. Völgyi, R. Ruiz, K. Box, J. Comer, E. Bosch and K. Takács-Novák, *Anal. Chim. Acta*, 2007, **583**, 418-428.
7. S. J. Gluck and J. A. Cleveland, *J. Chrom. A*, 1994, **680**, 43-48.
8. J. A. Cleveland, M. H. Benko, S. J. Gluck and Y. M. Walbroehl, *J. Chrom. A*, 1993, **652**, 301-308.
9. Y. Ishihama, M. Nakamura, T. Miwa, T. Kajima and N. Asakawa, *J. Pharm. Sci.*, 2002, **91**, 933-942.
10. Z. L. Ernst and J. Menashi, *Trans. Faraday Soc.*, 1963, **59**, 230-240.
11. P. C. Hidber, T. J. Graule and L. J. Gauckler, *J. Eur. Ceram. Soc.*, 1997, **17**, 239-249.
12. E. Furia and G. Sindona, *J. Chem. Eng. Data*, 2012, **57**, 195-199.
13. R. Porto, G. de Tommaso and E. Furia, *Ann. Chim.*, 2005, **95**, 551-558.
14. A. E. Martell, R. M. Smith and R. J. Motekaitis, 2001.
15. J. D. Sivey, J. S. Arey, P. R. Tentscher and A. L. Roberts, *Environ. Sci. Technol.*, 2013, **47**, 1330-1338.
16. J. D. Sivey, M. A. Bickley and D. A. Victor, *Environ. Sci. Technol.*, 2015, **49**, 4937-4945.
17. J. D. Sivey, C. E. McCullough and A. L. Roberts, *Environ. Sci. Technol.*, 2010, **44**, 3357-3362.
18. J. D. Sivey and A. L. Roberts, *Environ. Sci. Technol.*, 2012, **46**, 2141-2147.
19. S. S. Lau, S. M. Abraham and A. L. Roberts, *Environ. Sci. Technol.*, 2016, **50**, 13291-13298.